Science Robotics

robotics.sciencemag.org/cgi/content/full/2/8/eaan3028/DC1

Supplementary Materials for

A soft robot that navigates its environment through growth

Elliot W. Hawkes,* Laura H. Blumenschein, Joseph D. Greer, Allison M. Okamura

*Corresponding author. Email: ewhawkes@engineering.ucsb.edu

Published 19 July 2017, *Sci. Robot.* **2**, eaan3028 (2017)
DOI: 10.1126/scirobotics.aan3028

This PDF file includes:

Other Supplementary Material for this manuscript includes the following:
(available at robotics.sciencemag.org/cgi/content/full/2/8/eaan3028/DC1)

Movie S1 (.mp4 format). Lengthening.
Movie S2 (.mp4 format). Steering.
Movie S3 (.mp4 format). Constrained environments.
Movie S4 (.mp4 format). Forming structures from the body.

Text

Model for pressure-driven soft robot lengthening

The soft robot movement can be modelled as a quasi-static force balance where the driving force of movement is the internal pressure and the losses within the soft robot are opposing forces. This quasi-static approach is assumed due to the low inertia of the soft robot. The losses within the robot body result in a constant offset yield force, a viscous term as a function of rate, a Coulomb friction loss proportional to the straight length of the path, and a Capstan-like loss due to the curved length. The force balance equation is as follows, normalized by cross-sectional area:

$$P * A = F_y + \left(\frac{1}{\varphi} * r\right)^{1/n} * A + \mu_L * L_s + \sum_{L_c} C * e^{\mu_\kappa * \kappa * L_c},$$

where P is the internal pressure, A is the cross-sectional area at the tip, F_y is the yield force, r is the extension rate, φ is the extensibility (the inverse of viscosity), n is a power term close to unity, L_s is the length of straight sections, μ_L is the friction per unit length, L_c is the length of a curved section, κ is the path curvature for that section, μ_κ is the friction due to curvature, and C is a fitting term for the exponential. The yield force is related to the yield pressure through the cross-sectional area:

$$F_y = Y * A$$

This model was derived through a series of experiments to isolate each of the components and verify the predicted relationship to internal pressure. Each component was individually mitigated by lessening the contributing behavior of the soft robot, with the exception of the constant offset yield force, which was present in all tests.

Yield dependency. The constant offset, or yield, term was tested independently by slow lengthening over short straight sections (eliminating rate, length, and curvature dependencies). Two tests were performed to verify that yield remains constant over extension and is independent from the environment.

First, to determine the effects of environmental properties on lengthening (data shown in Fig. 4B of Manuscript), a soft robot body was extended through a gap (Fig. S1A). A soft robot body with inflated diameter of 2.5 cm was extended through a gap of height 2.2 cm and length 16.2 cm. The gap was lined with three materials to vary the surface interaction between the soft robot body and the environment: PTFE, textured neoprene rubber, and acrylic adhesive (Red-E Tape, True Tape, LLC). Pressure began low and was increased until movement began. Pressure was then modulated to keep the minimal constant speed of lengthening through the gap. The pressure (P) was recorded using a differential pressure sensor (PN: MPX5100DP) read by an Arduino UNO microcontroller. Displacement (d) was recorded using video capture of evenly spaced markers on the exterior of the soft robot body. The results of the test showed no relationship between surface material and the minimal pressure needed to extend.

To show that it is the yield force that remains constant, we varied the only other parameter present in the relationship, the cross-sectional area. To accomplish this, soft robot bodies were lengthened into a slanted gap (Fig. S1C). The pressure was incrementally increased until extension began. Then the robot body was allowed to grow until it no longer continued at the set pressure (P) due to the decreasing gap. A measurement was made of the achieved gap (h) and the pressure was incremented until

movement started again. This process was continued until 80% of bursting pressure was achieved. The experiment was performed with robot bodies with wall thickness 0.08 mm at three sizes: 2.6 cm, 4.8 cm, and 8.1 cm in free inflated diameter (D). At each size the slanted gap setup was adjusted to a starting gap of 80% free inflated size with a similar slope across setups. For a gap between two flat surfaces, we estimate the cross-sectional area as a shape with the height of the gap and the circumference of the free inflated tube (Fig. S1B). This results in the following formula for area:

$$A_{gap} = \frac{\pi}{4}h^2 + \pi\left(r - \frac{h}{2}\right) * h,$$

where A_{gap} is the cross-sectional area of the soft robot body within the gap, r is the free inflated radius of the tube and h is the gap height. The area was calculated from the measured height and the inverse of area was plotted against pressure (Fig. S2A). This revealed a directly proportional relationship between pressure and inverse area, the slope of which is the constant yield force.

Rate dependency. The rate dependency was measured in a test over a short straight section (data shown in Figure 3a of Manuscript). A soft robot body, approximately 1m long fully extended, was grown without external resistance. This length is small compared to the maximum length, so any length-based effects should be minimal, and the effect of turns should be negligible. A large pressure vessel was used to maintain a constant pressure during the test, without restricting the flow (Fig. S1D). The pressure within the vessel was increased to the test point pressure with the soft robot body kept from extending. The soft robot body was then released, and the movement was recorded by a high-speed overhead camera. The final pressure within the vessel was checked after the extension to verify small pressure loss. Pressures between the yield and the failure pressures were tested, and the average velocity of the movement was calculated from the high-speed video for each test. The rate was calculated by normalizing the velocity to the initial length of the soft robot body in this test, 0.5 m. In practice, this initial length can be made much shorter, as low as the length of the base, 0.28 m. The data follows the behavior of a Bingham plastic fluid (*34*):

$$r = \varphi * (P - Y)^n$$

with a yield pressure and a monotonically increasing relationship between pressure and extension rate. This is similar to the behavior describing plant cell growth in the Lockhart-Ortega model (*31*). Specifically, we match the extension of this model to linear rate made by Green (*34*), which is a simplification of Lockhart-Ortega when elastic stretching is small, osmotic flow is not limited, and growth is unidirectional as opposed to volumetric. When solved for pressure, the equation gives the first two terms in our model:

$$P = Y + \left(\frac{1}{\varphi} * r\right)^{1/n}$$

It is hypothesized that this viscoplastic relationship is due to losses arising from the material deformation during eversion at the tip, not losses due to fluid flow within the body or flow limit at the input. Increasing the diameter of the valve providing flow to the soft robot body had no effect on the rate of extension. Calculations of skin drag due to turbulent fluid flow indicate that at the Reynolds numbers of the tests lengths of over 30 m and flow rates of 8 m/s would be necessary to see any significant pressure drop over the length of the body. Conversely, when the thickness of the material was doubled, this

caused an increase in the yield pressure and a slight decrease in the extensibility, suggesting that the material properties determine the rate dependency.

Length dependency. The length dependency was determined through two tests. First, a max length test was performed to estimate the effect of length. To determine the maximum length a soft robot could reach, we placed a 10 cm diameter spool of polyethylene tubing (with 4.8 cm inflated diameter, 0.05 mm wall thickness) into the base. We then added air into the base, controlling the pressure to remain below 20 kPa. To control the pressure, measurements from the differential pressure sensor were used in feedback to command a proportional flow valve (PN: EC-P-05-6025). After the soft robot had grown to its full extent, using up all of the material on the spool, the length was measured (70 m) (Movie S1). The experiment was repeated when the robot passed through a small gap before extending. The same 4.8 cm inflated diameter tubing was extended through a 0.75 cm gap between two doors of a building. It then extended to its full length again (70 m), unaffected by the added obstacle of passing through a gap. The increase in length was not sufficient to raise the pressure needed to extend above the max containable pressure, indicating the dependency on length is small.

A second test was performed to find the relationship between pressure to grow and length. As previously discussed for the rate dependency, the skin drag within the soft robot is insignificant, so the length dependency must be related to the material flow within the soft robot body from base to tip. To isolate this phenomenon, a rigid tube with inner diameter equal to the free inflated diameter was lined with the material of the soft robot body, and a DC motor pulled additional thin-walled polyethylene tubing of the same diameter and thickness through the interior at a constant speed. The shear force on the rigid tube was measure by a six-axis force sensor (ATI Nano17) mounted between the rigid tube and stationary surface. The relationship between length of material in the tube and force is linear (Fig. S2B), indicating that the relationship between length and required pressure (beyond yield pressure) within the soft robot is linear as well.

Curvature dependence. To determine the effect of curved paths on the losses, soft robot bodies were extended between two curved surfaces (Fig. S1E) at a slow rate. A soft robot body with inflated diameter of 2.4 cm and wall thickness of 0.05 mm was used. The diameter of the setup (d_o) was varied between 17.4 cm and 29.8 cm. The pressure was incrementally increased until movement began. The soft robot body was allowed to grow until it could no longer continue at the current pressure (P) due to the total angle of previous curves in the path. The total angle was recorded and the pressure was incremented again. This procedure was repeated until a total angle of 7π radians or a total pressure of 33 kPa was achieved. The relationship between curved length and pressure (Fig. S2C) shows an exponential relationship with increasing curvature increasing the coefficient within the exponent. This behavior matches a modification of the capstan equation used to describe cable-conduit transmissions, treating the already inflated tube as a rigid stationary pulley and the new material inside as the tension rope around the stationary pulley, with the assumption of zero tension at the start of the soft robot body's path (*40*).

Natural system rate dependency data collection:

Data was collected from existing studies of natural biological systems for comparison to the pressure to rate relationship found for the soft robot system. Raw data for the proboscis extension in *Sipunculus nudus* came from Zuckerkandl (*27*). Points were collected from the plots using WebPlotDigitizer for each extension cycle. The time to extend the proboscis and the max pressure during extension were collected. For each extension, the length of the animal was assumed to double, giving a rate of one over the time to extend. The density of the coelomic fluid was assumed to be near fresh water density for pressure conversion. Yield pressure was reported by Zuckerkandl as 2 cm of H_20 and was subtracted out for plotting the data in Fig. 2.

Raw data for cell extension in *Nitella mucronata* was found in Green *et al.* (*34*). Again, points were collected using WebPlotDigitizer. The data was already in the proper format, pressure above yield and normalized rate, so no additional analysis steps were needed.

Demonstrations of lengthening soft robot capabilities

Here we describe the setup and soft robot parameters for each of the capabilities demonstrated in Figure 4 in the main text and in Movies S3,4.

Fig. 4A and Movie S3. A 2.4 cm diameter soft robot body moves through two eugenol glue boards facing one another, lightly touched together. Because material is added to the tip, the soft robot extends, despite the extremely sticky surface.

The same soft robot is extended through a 2.5 cm deep plastic container filled with polyvinyl acetate (white glue). An aluminum obstacle is placed over the container, forcing the soft robot body down into the glue. The soft robot body extends through the viscid glue, and does not drag the glue as it continues to extend, since the emerged soft robot body is static with respect to the environment.

The same soft robot body is lengthened through two arrays of steel nails, with the points of the nails facing toward one another. The nails are mounted into boards to hold them in place. The soft robot can potentially be used to access to remote locations in disaster scenarios, where they are likely to encounter sharp objects such as broken glass, pointed rubble, and splintery wood. Thus, the response of the soft robot to puncture is of significant concern. Although the soft robot body is an inflated tube, the pressures necessary for extend do not significantly deform the tube structure. Cracks propagate when the energy released by crack growth is larger than the energy required to form two new surfaces on either side of the crack (*41*). Because relatively little elastic energy is stored in the film of the tube, and because relatively more energy is required to form two new surfaces in polyethylene, small punctures do not propagate through the material and thus cause only minor pressure loss. This is in contrast to latex balloons, which fail catastrophically due to the large stored elastic energy and relatively small energy required to form two new surfaces in latex. Additionally, since the soft robot does not translate relative to the ground after extending, any debris that manages to puncture the body will remain in place, partially plugging any holes or gashes. This can be seen in the figure, as the nails partially plug their own holes.

An 8 cm diameter soft robot body is extended straight toward a 1 cm gap between two 3 cm thick planks of wood. The wood is covered on the end with white board for clarity of presentation. Because the lengthening body of the soft robot is almost entirely air, it can easily deform into small gaps. The rigid, bulky components of the base remain behind.

Figure 4b. See Section Model for pressure-driven soft robot lengthening**,** *Yield Dependency* for details.

Figure 4c and Movie S4. A 2.4 cm diameter soft robot is extended under a standard door with less than 1 cm gap between the floor and door. The soft robot lengthens across the room (a distance of 2 m) before going under a pipe and up to a valve. The soft robot then grows into a hook shape at its end, just over the valve. When tension is applied to the film that is inside the soft robot passing toward the tip, the hook tightens around the valve. With increased tension, the soft robot shortens, turning the valve. The torque required to turn the valve is 0.9 Nm. The ability to access locations beyond where the main body can go allows a powerful motor to be used to turn the valve, even though the motor cannot access the valve. The motor remains in the bulky base outside the room, while the light, mobile tip extends into the room and to the valve.

A 2.4 cm diameter soft robot is extended to a fire through model roof rafters made of wood. The soft robot is filled with an air/water mixture. The fire is made by inserting a number of wicks into a pool of liquid wax. When the soft robot crosses the fire, the polyethylene film melts and the pressurized air/water mixture sprays through the created hole in the robot body wall to put out the fire. Other contents, such as CO_2 foam, could be used as well.

An 8 cm diameter soft robot body is extended into a helix to construct a radio frequency antenna. The polyethylene tubing is metalized along a strip to transmit the signal. The antenna is modeled using Ansoft (Fig. S3). A plot showing how much power is reflected from the antenna (S11, or return loss) over a sweep of frequencies shows that the return loss is below -10 dB for nearly the entire range of 250-500 MHz.

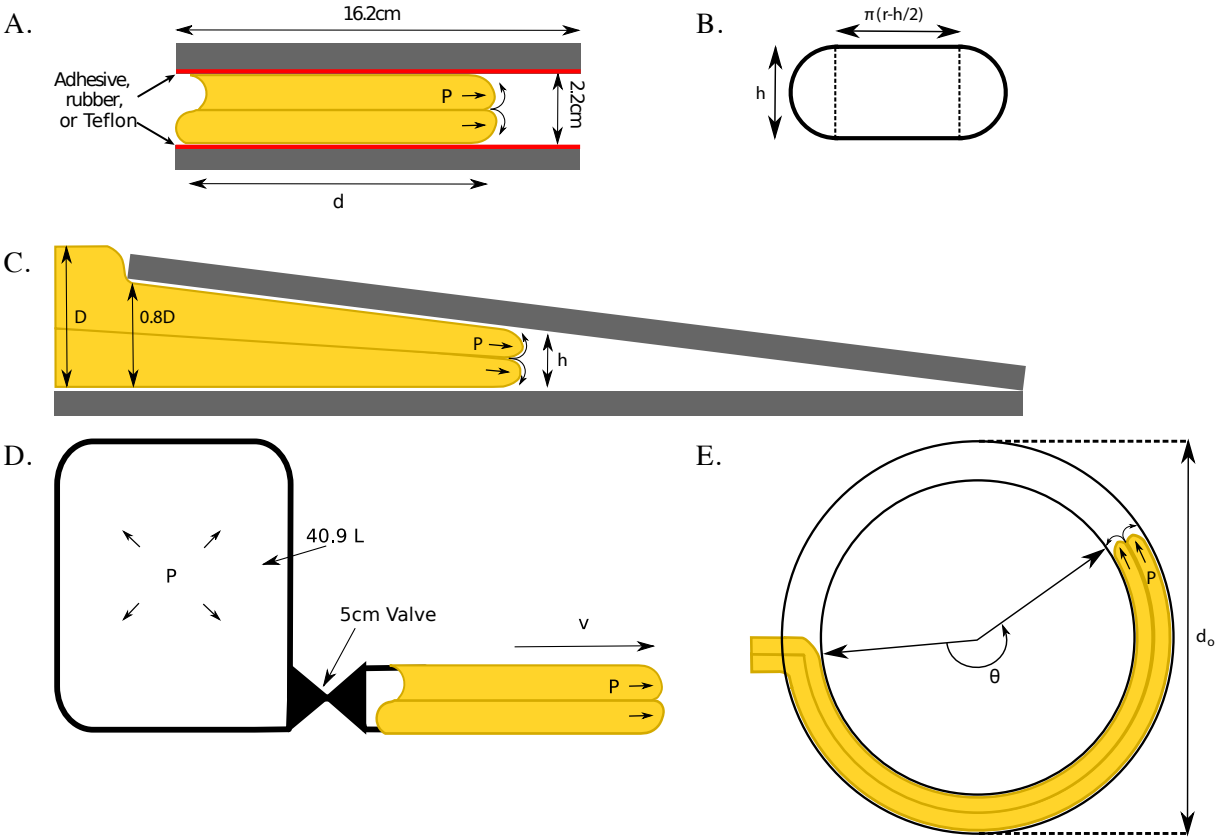

Fig. S1. Experimental arrangement for collection of data shown in Figs. 2 and 4 and fig. S2. (**A**) To determine the relationship between force required to move and environmental factors, a soft robot body was extended through a gap, where d is the distance travelled and P is the extension pressure. The gap was coated with one of three materials to determine the effect of surface properties: acrylic adhesive, rubber, or PTFE (Teflon). (**B**) The model for predicting the relationship between pressure to extend and area while extending into a gap uses the real cross-sectional area of the tubing in the gap, represented here schematically. r is the free inflated radius of the tube (equal to $D/2$) and h is the gap height. (**C**) To determine the relationship between pressure to extend and size of the gap, a soft robot body was extended into a gap of decreasing size, where D is the diameter of the unconstrained tubing, P is the extension pressure, and h is the height of the gap at the tip of the soft robot. This was repeated with tubing of varying diameter. (**D**) To determine the relationship between pressure to extend and extension speed, a soft robot body was extended from a large pressure vessel to remove flow restrictions and maintain constant pressure. (**E**) To determine the relationship between pressure to extend and curved extension paths, a soft robot body was extended into a constant gap with a set curvature, where θ is the total angle through which the soft robot body has extended, P is the extension pressure, and d_o is the diameter of the outer wall constraining extension direction. This was repeated with gaps of varying diameter.

A.

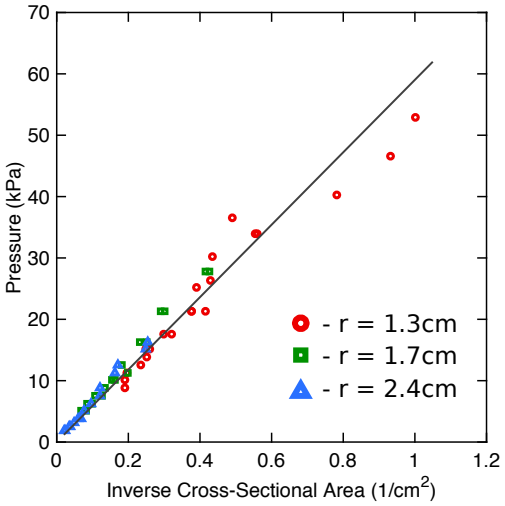

B.

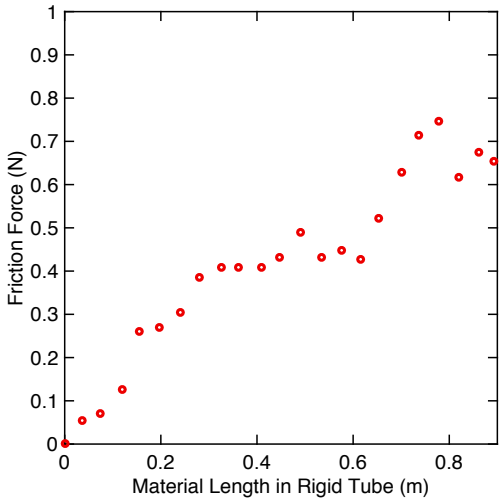

C.

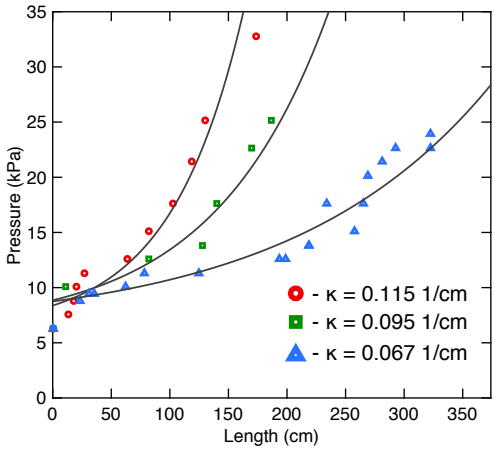

Fig. S2. Additional experimental results from tests to determine full model for soft robot lengthening. (**A**) One over the cross-sectional area as a soft robot body is extended into a gap plotted against the pressure necessary to extend with that reduced area. Data is shown for three values of robot body radius. Linear relationship indicates a constant offset force needed to begin extension. (**B**) Friction force due to thin-walled polyethylene tubing being pulled through a tube lined with polyethylene. Force is plotted versus the length of material, showing a linear relationship with length. This indicates a friction force is present in the soft robot extension model based on the length of the material flow within the soft robot body. (**C**) Length of curved section versus pressure to extend, plotted for three different curvatures. Bottom line shows the previously established friction due to length alone at this scale. Data follows an exponential trend with length, with the exponent coefficient a function of the curvature. This behavior mirrors the Capstan equation as applied to cable-conduit transmissions.

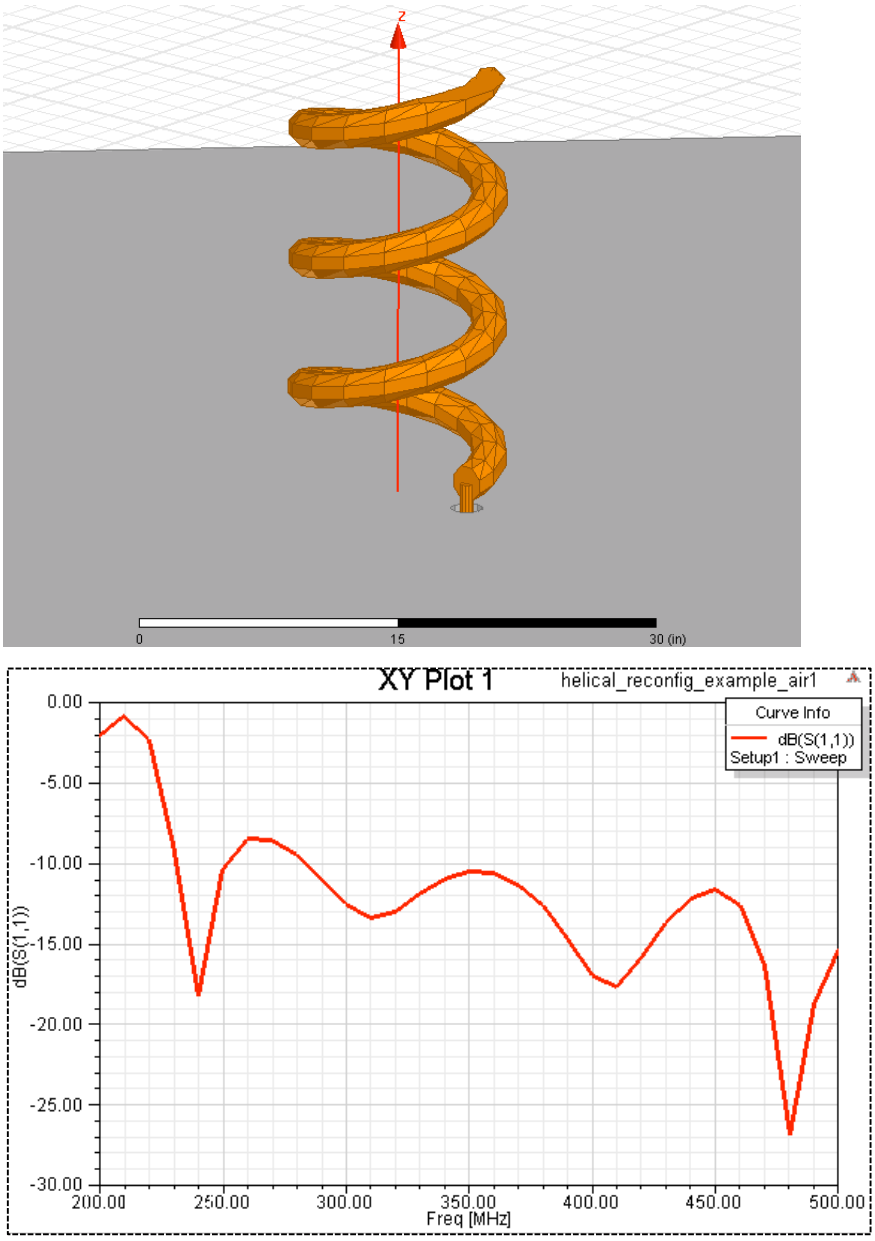

Fig. S3. Modeling of a helical antenna formed with a soft robot. *Top:* 3D model of antenna (Ansoft, LLC). *Bottom:* Modeled S11, or return loss, showing that the return loss is below -10 dB for the majority of the range from 250-500 MHz.

Fig. S4. Extension of a soft robot body with preset pattern of branching. Multiple branches can be preprogrammed at time of manufacture.

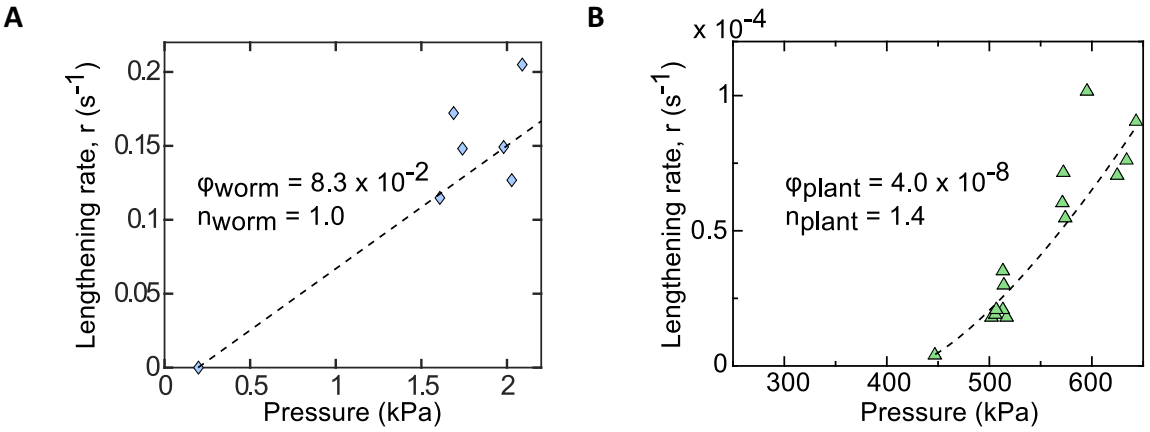

Fig. S5. Viscoplastic relationships for natural extending systems. (**A**) Lengthening rate of proboscis versus internal body pressure for *Sipunculus nudus* collected from Zuckerkandl. (**B**) Lengthening rate of cell versus turgor pressure for *Nitella mucronata* collected from Green *et al.*

Movie S1. Lengthening.
Slow Lengthening and Retraction: Robot body extending using compressed air.
72m Lengthening: A soft robot with an 8 cm diameter body is extended from a 28 cm long base to a full length of 72 m. The material for the body is initially spooled inside of the base.

High-speed Lengthening: A 2.4 cm diameter soft robot body is extended at high speed across a horizontal surface toward an array of wooden blocks. The white tape markers are placed one meter apart. The soft robot body covers the meter in 0.183 s at an average speed of 5.5 m/s. Further, it passively negotiates through the blocks of wood.

Movie S2. Steering.

Soft robot turning: Control of the pressure in the side chambers of the robot controls turning direction (Fig. 3A-D and Fig. 5). When the upper chamber is pressurized, the upper side of the robot lengthens in the region of material that is at the tip, and a turn downwards is commanded. When the lower chamber is pressurized, the opposite occurs. A camera is mounted to the front of the robot to allow sensing of the environment. The camera is held in place by the tension in a cable running from the camera through the body of the robot.

Navigating to a light: Closed-loop control enables the robot to navigate toward a target, here a lightbulb. The target is placed in two different locations, and the same robot forms itself into the shape that reaches the target. Inset in the upper right is a point of view video from the camera on the tip of the robot. The image is corrected to maintain upright orientation. See supplementary text for more details.

Movie S3. Constrained environments.

Lengthening through fly paper, glue, and nails: See supplementary text for details.

Ice (as part of sequence of constrained environments, occurring after nails): A 2.4 cm diameter soft robot body is extended vertically up a sheet of ice. Because it is anchored below, it can climb slippery surfaces up until heights when the structure begins to buckle.

Lengthening Across Water: A 4.8 cm diameter soft robot body is extended across a pond of water with an active fountain disturbing the water. The water surface is roughly 20 cm below the edge of the pond. Lengthening across water is possible because the soft robot body transmits forces back to the section that is anchored on the ground.

Smooth Vertical Surface: A 2.4 cm diameter soft robot body is extended vertically up a smooth metal surface. Small tendrils, coated with acrylic adhesive (TrueTape, LLC) emerge from the tip of the soft robot body during extension and bond to the surface. Because the body does not move with respect to the surface, the adhesive can be permanent, not requiring controllable adhesive like that used by legged wall-climbing robots.

Movie S4. Forming Structures from the Body.

Active Hook Under Door: See supplementary text for details.

Lengthening Through a Drop Ceiling: A 4.8 cm diameter soft robot is extended through a drop ceiling, filled with air ducts, wiring, light fixtures and other obstacles. The soft robot is able to extend 10 m and emerge from a removed ceiling tile, pulling a wire through its body. This demonstrates the ability to route cables through such environments. While this soft robot was lengthened open loop, it is possible to attach a camera to the end of the soft robot such that during extension the camera is moved forward at the extension rate. This would allow a user to potentially steer the soft robot through a disaster scenario using visual feedback from the tip.

Extension into At-Scale Brain Ventricle: A 5 mm diameter soft robot body is extended through an at-scale model brain ventricle. The ventricle is 3D printed in plastic (Polylactic acid) from a CT scan of an adult human's brain. While air is used to extend the soft extending catheter in the figure, hydraulic powered extension has also been tested for potential use *in vivo* (using saline solution). Because the soft extending catheter extends from the tip, rather than sliding like all current catheters, there are no shear frictional forces with the tissue. After full extension, a radiofrequency (RF) ablation tool is passed through the center of the catheter, inside the internal layer of film that is passing toward the tip. The tool is 0.8 mm in diameter. The tool is then retracted, and the catheter is depressurized and retracted, now a soft, limp plastic bag. The soft extending catheter uses 10 micrometer thick polyethylene tubing. The catheter is then extended in free space, and the shape of the soft extending catheter remains the same as when extending inside the model brain. This is because the shape is predetermined before extension by presetting the shape during manufacture (from the scan of the patient's brain). Because the shape of the catheter matches the cavity in the brain, there are no normal contact forces required for the soft extending catheter to reach it desired end configuration. This could be a critical advance in brain catheters, as neurosurgeon consultants say that current catheters apply force to brain tissue, causing damage during surgery. Because of the delicate nature of the brain tissue, memory loss can be caused by these normal contact forces.

Pneumatic Jack: An 8 cm diameter soft robot is extended under a crate that is resting on a foam ball. The soft robot extends into a spiral, and once fully extended, inflates at 25 kPa to lift the crate. This pneumatic jack can lift over 150 kg.

Fire Hose: See supplementary text for details.

Antenna: See supplementary text for details.